NASA Technical Note D-7217

Subsonic Wind-Tunnel Tests of a Trailing-Cone Device For Calibrating Aircraft Static Pressure Systems

S083N(NC)

Military fighter, helicopter, business jet, and UAV examples
of SpaceAge Control air data products in use.

SpaceAge Control

For other technical papers such as those listed below, visit:

http://spaceagecontrol.com/litroom.htm#B

- *Airdata Measurement and Calibration* (TM 104316)
  - air data measurement methods; includes references and bibliography
- *Measurement of Static Pressure on Aircraft* (Report 1364)
  - detailed information on how to mount air data booms
- *Airdata Calibration of a High-Performance Aircraft for Measuring Atmospheric Wind Profiles* (TM 101714)
  - how to maximize air data accuracy from air data booms.
- *Investigation of the Fuselage Interference on a Pitot-Static Tube Extending Forward From the Nose of the Fuselage* (TN1496)
- *Accuracy of Airspeed Measurements and Flight Calibration Procedures* (Report 919)
- *Wind-Tunnel Calibration of a Combined Pitot-Static Tube and Vane-Type Flow-Angularity Indicator at Mach Numbers of 1.61 and 2.01* (TN 3808)
- *The Measurement of Air Speed in Airplanes* (TN 616)
- *Summary of Methods of Measuring Angle of Attack on Aircraft* (TN 4351)
- *Measurement of Aircraft Airspeed and Altitude* (RP 1046)
- *Position Error Calibration of a Pressure Survey Aircraft Using a Trailing Cone* (TN-313)

For information air data products that measure total pressure, static pressure, outside air temperature (OAT), total air temperature (TAT), angle of attack (AOA, alpha), and angle of sideslip (AOS, beta), contact us:

SpaceAge Control
38850 20th Street East ◆ Palmdale, CA 93550 USA
www.spaceagecontrol.com ◆ email@spaceagecontrol.com
661-273-3000 ◆ 661-273-4240 (fax)

SUBSONIC WIND-TUNNEL TESTS OF A TRAILING-CONE DEVICE FOR CALIBRATING AIRCRAFT STATIC-PRESSURE SYSTEMS

By Frank L. Jordan, Jr., and Virgil S. Ritchie
Langley Research Center

SUMMARY

A trailing-cone device for calibrating aircraft static-pressure systems was investigated by means of limited aerodynamic tests in a transonic wind tunnel. The tests were conducted at Mach numbers from 0.30 to 0.95 with Reynolds numbers from 3.0×10^6 to 13.4×10^6 per meter (0.9×10^6 to 4.1×10^6 per foot).

The principal objective of the tests was to investigate the pressure-sensing characteristics of the trailing-cone device with pressure-tube orifices at several locations ahead of the cone and including (for a near-optimum location of tube orifices) the interference of a tube-protection skid. Related measurements of secondary interest included the drag of the entire trailing-cone system as well as momentary inclinations and vertical locations of the pressure tube of the device.

Test results indicated that differences between trailing-cone and free-stream static pressures varied consistently with distance between the tube orifices and the cone, as expected, but that these differences were generally small. A trailing-cone configuration with a tube-protection skid and with tube orifices located 5 cone diameters ahead of the cone vertex indicated pressures which were less than free-stream static pressure by about 0.016 percent and 0.063 percent at Mach numbers of 0.30 and 0.95, respectively. These small static-pressure differences were about 0.25 percent and 0.08 percent of the impact pressure and corresponded to Mach number differences of less than 0.0004 and 0.0006 at Mach numbers of 0.30 and 0.95, respectively.

Differences between device-indicated and free-stream static pressures were not greatly influenced by a protection skid at the downstream end of the pressure tube of the device nor by a 2-to-1 change in test Reynolds number.

INTRODUCTION

Flight calibration of the static-pressure systems of aircraft is essential to the accurate determination of airspeed, altitude, and Mach number. Such calibration involves precise resolution of the difference between the pressure indicated by the static system of

the aircraft and the true ambient pressure. The determination of this pressure difference (generally known as static-system position error) throughout the aircraft flight envelope can be complicated, time consuming, and expensive.

Various methods are available for obtaining in-flight calibrations. (See refs. 1 to 3.) One method involves the use of a trailing static-pressure device. Such devices are trailed from the test aircraft at a sufficient distance to minimize the effects of the aircraft disturbance field. A differential-pressure gage is used to directly measure the difference between pressures sensed by the trailing static device and the aircraft static system. Early trailing static devices required calibration, however, and were aerodynamically unstable at transonic speeds (ref. 4).

A more recent trailing static-pressure device, which utilizes the drag of a perforated cone for improved aerodynamic stability (refs. 5 to 13), eliminates the problems associated with earlier trailing static devices. The trailing-cone system consists of a light fiber-glass cone towed behind the test aircraft; this system utilizes a relatively long tube incorporating static-pressure orifices located an appropriate distance ahead of the cone.

Most trailing-cone investigations (refs. 5 to 12) indicate that properly designed devices are aerodynamically stable over a wide range of flight conditions and are capable of indicating pressures very near free-stream static (ambient) pressure. The trailing-cone technique, therefore, is viewed as a method for quick and economical calibration of aircraft static-pressure systems and has been recommended for further use (refs. 8, 9, 10, and 12).

The purpose of this report is to present the results of limited subsonic wind-tunnel tests of a trailing-cone device. The tests were conducted primarily to determine the pressure-sensing characteristics of the device in connection with an evaluation of the trailing-cone technique. The trailing cone used for the present tests was supplied by the Federal Aviation Administration (FAA). This device differs in some respects from trailing-cone systems currently in use (ref. 11).

SYMBOLS

Test-related quantities are given in both SI and U.S. Customary Units; the latter units were used for measurements and calculations.

A area of trailing-cone base, 126.68 cm^2 (19.63 in^2)

C_D total drag coefficient, $\frac{\text{Drag}}{q_\infty A}$

c_p specific heat at constant pressure

c_v specific heat at constant volume

D base diameter of trailing cone, 12.70 cm (5.00 in.)

h_p pressure altitude (for standard atmospheric conditions) corresponding to free-stream static pressure, m (ft)

Δh_p pressure-altitude error (for standard atmospheric conditions), m (ft)

M_∞ free-stream Mach number

ΔM Mach number error corresponding to static-pressure error

p static pressure, N/m^2 (lb/ft^2)

p_t total pressure, N/m^2 (atm)

p_∞ free-stream static pressure, N/m^2 (lb/ft^2)

q_c free-stream impact pressure, $p_t - p_\infty$, N/m^2 (lb/ft^2)

q_∞ free-stream dynamic pressure, $\frac{\gamma}{2} p_\infty M_\infty^2$, N/m^2 (lb/ft^2)

R Reynolds number per meter (per foot)

x axial distance between center of pressure-tube orifices and apex of trailing cone, cm (in.)

y vertical distance between tube pressure orifices and test-section center line (negative values denote tube locations below center line), m (in.)

α angle of attack of static-pressure tube, deg

γ ratio of specific heats, $c_p/c_v = 1.400$

APPARATUS AND TESTS

Trailing-Cone Device

Principal details of the trailing-cone device and its components are shown in figure 1. These include assembly views of the device without and with a skid for protecting the device pressure tube (fig. 1(a)), details of the cone and pressure tube (fig. 1(b)), and details of the tube-protection skid (fig. 1(c)). The cone is a lightweight shell constructed of fiber glass (figs. 1(a) and 1(b)); it has a base diameter of 12.70 cm (5.00 in.) and an included angle of about 32°. Twelve holes, each 2.54 cm (1.0 in.) in diameter, are located in the surface of the cone as shown in figure 1(b).

For flight and wind-tunnel tests, the cone is trailed at the end of 0.635-cm-diameter (0.250-in.) nylon pressure tubing containing a high-strength steel wire to support drag loads. The steel wire is attached to pressure unions at both ends of the nylon tubing. At the cone the union is retained by a conical nylon bushing within the apex portion of the fiber-glass cone (fig. 1(b)); the nylon bushing contains a steel bearing insert which permits rotation of the cone independent of the nylon tubing and wire.

At a suitable location ahead of the cone, a stainless-steel pressure-sensing tube 50.80 cm (20.00 in.) long (fig. 1(b)) is inserted as a part of the pressure-tubing system. The outside diameter of the steel tube is 0.729 cm (0.287 in.), and that for the nylon tubing is 0.635 cm (0.250 in.). The steel pressure tube contains 48 individual orifices of 0.0635-cm (0.025-in.) diameter arranged in four rings located 1.27 cm (0.50 in.) apart; the 12 orifices in each ring are circumferentially spaced 30° apart. All orifices open into a common averaging chamber inside the pressure tube.

Tube-Protection Skid

Figure 1(c) shows details of an NASA designed wire skid for protecting the steel pressure tube from possible damage when the trailing-cone system is dragged on runway surfaces during take-off and after landing operations. This tube-protection skid attaches to the downstream end of the pressure tube (figs. 1(a) and 1(c)). The skid is constructed of 0.318-cm-diameter (0.125-in.) stainless-steel wires silver-soldered to a short length of stainless-steel tubing having an outside diameter of 0.729 cm (0.287 in.).

Test Arrangements

The several trailing-cone configurations tested are illustrated in figure 2. The axial distances between the pressure-tube orifices and the cone apex for the test configurations are given in terms of cone base diameters and in centimeters (inches). Only the test configuration with orifices located 5 cone diameters ahead of the apex of the cone employed the tube-protection wire skid, as shown.

Principal details of the test arrangement in the wind tunnel are shown in figure 3. The cone was tested at the downstream ends of tubing-wire systems about 23.5 to 24.4 meters (77 to 80 ft) long. The upstream ends of the tubing-wire systems were fastened to an axial-force balance secured to the guide vanes in the tunnel low-speed section. A T-union was inserted into the nylon tubing at the balance-tubing juncture for ducting the device-sensed pressures to the measurement transducer.

Thin, cable-supported rings employed for centering the tubing at two locations upstream of the test section are illustrated in figure 3. The diameter of the upstream centering ring (in the low-speed section) was 15.24 cm (6.0 in.); the diameter of the centering ring located about 6.0 meters (19.8 ft) ahead of the pressure-sensing tube was 2.54 cm (1.0 in.).

Wind Tunnel and Test Conditions

The present tests were conducted in the Langley 8-foot transonic pressure tunnel (ref. 14). This single-return tunnel has a rectangular test section with slotted top and bottom walls to permit continuous operation through the transonic speed range. The cross-sectional area of the test region is approximately 4.65 meters^2 (50 ft^2). Tunnel controls allow for the independent variation of Mach number, pressure, temperature, and specific humidity.

Tests were conducted at Mach numbers from 0.30 to 0.95 at tunnel total pressures of 101 325 and 50 662 N/m^2 (1.0 and 0.5 atm). Test Reynolds numbers and simulated pressure altitudes are shown in figure 4. The total temperature of the tunnel air was automatically controlled at approximately 322 K (120° F). Dewpoints were maintained near 250 K (-10° F) during the tests to minimize the possibility of humidity effects.

Observations, Measurements, and Accuracy

Visual observations of the trailing-cone systems were made during tests, and schlieren photographs were obtained to record momentary inclinations (angles of attack) and vertical locations of the static-pressure tube. The accuracies of the pressure-tube inclinations and vertical locations, measured from the schlieren photographs, are estimated to be about 0.3° and 2.54 cm (1.0 in.), respectively.

An axial-force balance having a range of 444.8 N (100 lb) was used to measure drag loads of the trailing-cone systems. The estimated accuracy of this balance was about 4.45 N (1.0 lb). Free-stream dynamic pressure at the pressure-tube location, instead of that at the cone location, was used for reducing the data to coefficient form. A differential-pressure transducer was used to measure differences between the pressure indicated by the trailing-cone system and the tunnel reference static pressure. This transducer had a range of 3.45 kN/m^2 (0.5 lb/in^2) and an estimated accuracy of

0.5 percent of the full range. Tunnel reference static and total pressures were measured by absolute manometers having accuracies of about 19 N/m^2 (0.4 lb/ft^2).

Estimated possible inaccuracies in pressure measurements at a total pressure of 1.0 atm could produce static-pressure errors as large as 0.51 percent and 0.03 percent of the impact pressure at the limiting Mach numbers of 0.30 and 0.95, respectively; such estimated inaccuracies do not include possible small uncertainties in tunnel calibration. These possible static-pressure errors correspond to altitude uncertainties of about 3 meters (10 ft) or less, at the simulated pressure altitudes, for standard atmospheric conditions. Possible errors in pressure measurements at a tunnel total pressure of 0.5 atm could permit pressure-coefficient and pressure-altitude uncertainties about twice as large as those at a total pressure of 1.0 atm.

RESULTS AND DISCUSSION

General Behavior and Oscillation of Trailing-Cone Device

Visual observations of the general behavior of the trailing cone during the tests revealed that the cone lifted off the test-section floor at Mach numbers near 0.2 and gradually approached the test-section center line as Mach number and dynamic pressure were increased. The cone and the pressure tube were observed to oscillate in a manner which appeared to be random. Specific reasons for the cone and tube oscillations are not known, but the oscillations may have been related to tunnel turbulence (including possible flow disturbances from the nearest upstream tube-centering ring) and other factors including possible instability of the cone tubing system.

Vertical Location and Inclination of Pressure Tube

Pressure-tube vertical locations.- Figure 5 shows pressure-tube momentary locations (from numerous schlieren-photograph measurements), which generally corroborate the previously described visual observations of pressure-tube oscillation during wind-tunnel tests. These data reveal pressure-tube vertical excursions as large as ±0.1 meter (±4.0 in.) at Mach numbers from 0.60 to 0.95. The data include only the several momentary tube locations measured over test periods of a few minutes duration, however, and are not intended to define the maximum amplitude of tube oscillation.

The faired lines in figure 5 are intended to show only general trends of tube location for the test conditions. The data show that for a total pressure of 1.0 atm, tube locations varied from about 0.44 to 0.06 meter (17.3 to 2.4 in.) below the test-section center line at Mach numbers of 0.30 and 0.95, respectively. The data also indicate that for a total pressure of 0.5 atm, at the higher test Mach numbers, the pressure-tube location below the test-section center line is about twice that for a total pressure of 1.0 atm.

Pressure-tube inclinations.- Figure 6 shows pressure-tube momentary angles of attack indicated by numerous schlieren-photograph measurements. The pressure-tube angle of attack varied from about 3.5° at a Mach number of 0.30 (at a total pressure of 1.0 atm) to approximately 0° at Mach numbers from about 0.60 to 0.95. Indicated angle-of-attack variations of as much as $\pm 0.5^{\circ}$ at some test Mach numbers are believed to result partly from measurement inaccuracies and partly from momentary tube inclination changes induced by cone motions. Schlieren photographs indicated momentary bending of the nylon tubing between the pressure tube and the cone.

Pressure-Sensing Characteristics of Trailing-Cone Device

Differences between pressures indicated by the tested trailing-cone device and free-stream static pressure are presented in figures 7 to 9. The variation of pressure differences $\left(\text{in the coefficient forms } \frac{p - p_\infty}{q_c} \text{ and } \frac{p - p_\infty}{p_\infty}\right)$ with Mach number is shown in figures 7 and 8; these figures include lines for interpreting the pressure differences in terms of corresponding differences in Mach number and pressure altitude (standard atmospheric conditions). Figure 9 shows the variation of $\frac{p - p_\infty}{q_c}$ with distance between the apex of the perforated cone and the pressure-tube orifices. This figure includes lines indicating the estimated limits of data scatter due to possible errors in pressure measurement; these estimates do not include possible additional scatter related to small uncertainty in the tunnel calibration.

The data in figures 7 to 9 reveal that the pressures indicated by all the tested trailing-cone configurations are generally near the free-stream static pressure; the maximum differences between trailing-cone and free-stream Mach numbers did not exceed about 0.003. The data in figures 7 to 9 also indicate an expected trend in which the trailing-cone pressures increased slightly but consistently as the distance between the pressure-tube orifices and the apex of the cone was decreased from 10 to 4 cone diameters. The data indicate that at the higher test Mach numbers, the trailing-cone pressures were larger than free-stream values when pressure orifices were located only 4 cone diameters ahead of the apex of the cone (fig. 9); such pressure differences could be expected to become even larger at higher subsonic speeds.

Differences between trailing-cone and free-stream Mach numbers were very small for test configurations having pressure orifices located ahead of the apex of the cone by 5 and 6 cone diameters. The configuration for $x/D = 5$ (with tube-protection skid attached) indicated pressures which were less than free-stream static pressure by amounts varying from 0.25 percent to 0.08 percent of the impact pressure (fig. 7(a)), or from 0.016 percent to 0.063 percent of the static pressure (fig. 7(b)), at Mach numbers of 0.30 and 0.95, respectively. These small pressure differences correspond to Mach

number differences of less than 0.0004 and 0.0006 at Mach numbers of 0.30 and 0.95, respectively, and to pressure-altitude differences near 3 meters (10 ft).

The present data reveal an apparent tendency for the trailing-cone device to indicate pressures slightly less than free-stream static pressure when pressure-tube orifices were located ahead of the apex of the cone by 5 or more cone diameters. This may be related to possible effects of observed pressure-tube inclinations and oscillations as well as to possible tunnel calibration uncertainties. Estimates based on data reported in reference 15 indicate that effects of tube inclinations of about 3.5° at $M_{\infty} = 0.30$ and 0.5° at $M_{\infty} = 0.95$ can reduce tube-indicated pressures by $\frac{p - p_{\infty}}{q_c}$ values of about 0.0022 and 0.0005, respectively. Such effects of tube inclination are sufficient to account for a large portion of the indicated low trailing-cone pressures except for some data points for the $x/D = 10$ configuration at test Mach numbers near 0.90 and 0.95. (See fig. 7.) These latter pressure differences are believed to be considerably larger than combined effects of tube inclination and possible tunnel calibration uncertainties.

Comparison of data from tests of trailing-cone configurations with $x/D = 4$ and $x/D = 6$ at a total pressure of 1.0 atm (fig. 7) with data from tests at a total pressure of 0.5 atm (fig. 8) indicates that the pressure-sensing characteristics of the trailing-cone device were not changed greatly by a 2-to-1 variation of the test Reynolds number.

The present data for the tested trailing-cone configurations generally indicate that such devices are capable of sensing pressures very near the free-stream static pressure at subsonic speeds if pressure-tube orifices are located about 5 to 6 cone diameters ahead of the apex of the cone. Pressure-sensing characteristics superior to those presently reported may possibly be afforded by trailing-cone devices incorporating various system improvements, such as increased cone diameter. However, realization of the full pressure-sensing accuracy of such devices during flight applications necessitates proper installation of the device and trailing it sufficiently far behind the aircraft where the disturbance-field pressure is essentially the same as ambient pressure. Established procedures for trailing-cone applications are described in reference 11.

Drag Characteristics

Drag characteristics of the tested trailing-cone configurations are presented in figure 10. Although the drag coefficients shown were based on free-stream conditions, the usefulness of the data is limited to some extent because only the downstream portion (including cone and pressure tube) of the entire trailing-cone system was located in the test section of the wind tunnel. However, this limitation should not apply to the indicated drag increment produced by the tube-production skid.

CONCLUSIONS

Aerodynamic tests of a trailing-cone device in the Langley 8-foot transonic pressure tunnel at Mach numbers from 0.30 to 0.95 with Reynolds numbers up to 13.4×10^6 per meter (4.1×10^6 per foot) yielded the following pressure-sensing characteristics applicable for the test conditions:

1. The pressure indicated by the tested device increased slightly but consistently as the distance between the trailing cone and the pressure-tube orifices was decreased from 10 to 4 cone diameters.

2. A test configuration with tube orifices located 5 cone diameters ahead of the cone and with a tube-protection skid indicated pressures less than free-stream static pressure by about 0.016 percent and 0.063 percent of the static pressure, or by about 0.25 percent and 0.08 percent of the impact pressure, at Mach numbers of 0.30 and 0.95, respectively. These small pressure differences corresponded to Mach number differences of less than 0.0004 and 0.0006 at Mach numbers of 0.30 and 0.95, respectively.

3. An apparent tendency for the tested device to indicate pressures slightly less than free-stream static pressure when pressure-tube orifices were located ahead of the cone by 5 or more cone diameters may have been related to effects of observed tube inclinations and oscillations as well as to possible small tunnel calibration uncertainties.

4. The pressure-sensing characteristics of the trailing-cone device were not greatly influenced by a 2-to-1 change in test Reynolds numbers.

5. A protection skid at the downstream end of the pressure tube of the device produced an increment in the drag of the entire system, but it did not greatly affect the pressure-sensing characteristics of the device.

Langley Research Center,
National Aeronautics and Space Administration,
Hampton, Va., March 16, 1973.

REFERENCES

1. Herrington, Russel M.; Shoemacher, Paul E.; Bartlett, Eugene P.; and Dunlap, Everett W.: Flight Test Engineering Handbook. AFTR No. 6273, U.S. Air Force, May 1951 (revised Jan. 1966). (Available from DDC as AD 636 392.)

2. Deleo, Richard V.; Cannon, Peter J.; and Hagen, Floyd W.: Evaluation of New Methods for Flight Calibration of Aircraft Instrument Systems. Pt. 1: Analysis of Altimeter, Airspeed and Free-Air-Temperature Systems. WADC TR 59-295 Pt. I, U.S. Air Force, June 1959. (Available from DDC as AD 239 767.)

3. Huston, Wilber B.: Accuracy of Airspeed Measurements and Flight Calibration Procedures. NACA Rep. 919, 1948. (Supersedes NACA TN 1605.)

4. Smith, K. W.: The Measurement of Position Error at High Speeds and Altitude by Means of a Trailing Static Head. C.P. No. 160, Brit. A.R.C., 1954.

5. Shrager, Jack J.: Test of Trail Cone System To Calibrate Static Parts for Barometric Altimeters. Rep. No. RD-64-156, FAA, Dec. 1964. (Available from DDC as AD 611 444.)

6. Mickle, Don A.; and Soderquist, Robert H.: Trailing Cone Method of Measuring Static Source Position Error, Evaluation and Calibration Phase – First Interim Report. Rep. No. FT2123-56R-64, U.S. Nav. Air Test Center (Patuxent River, Md.), Aug. 17, 1964. (Available from DDC as AD 445 714.)

7. Rhodes, William B.: Measurement of Static Pressure in Flight by Trailing-Cone Static Source Method. Naval Weapons Bull. No. 2-65, Apr.-June 1965, pp. 23-25.

8. Barnes, C. S.: Flight Assessment of a Douglas Trailing-Cone Static-Pressure Probe at Subsonic Speeds. Tech. Rep. 69139, Brit. R.A.E., July 1969.

9. Ikhtiari, Paul A.; and Marth, Verlyn G.: Trailing Cone Static Pressure Measurement Device. J. Aircraft, vol. 1, no. 2, Mar-Apr. 1964, pp. 93-94.

10. Watson, E. T., Jr.: Trailing Cone Reference System. Summary of Independent Developmental Research Efforts, Rep. No. DEV-3674, Douglas Aircraft Co., Nov. 30, 1964.

11. Crowley, L. D.: Trailing Cone Systems Applications. TM-GEN-4158 Douglas Aircraft Co., Aug. 7, 1967.

12. Russell, William M.: Trail Cone Static System Calibration Technique. 16th Technical Conference, Vol. 2, Int. Air Transport Assoc., 1965, WP-105.

13. Shrager, Jack J.: Limited Survey of Commercial Jet Aircraft Altimeter System Position Error by Pacer With Trailing Cone. Rep. No. RD-64-157, FAA, Dec. 1964.

14. Schaefer, William T., Jr.: Characteristics of Major Active Wind Tunnels at the Langley Research Center. NASA TM X-1130, 1965.

15. Ritchie, Virgil S.: Several Methods for Aerodynamic Reduction of Static-Pressure Sensing Errors for Aircraft at Subsonic, Near-Sonic, and Low Supersonic Speeds. NASA TR R-18, 1959.

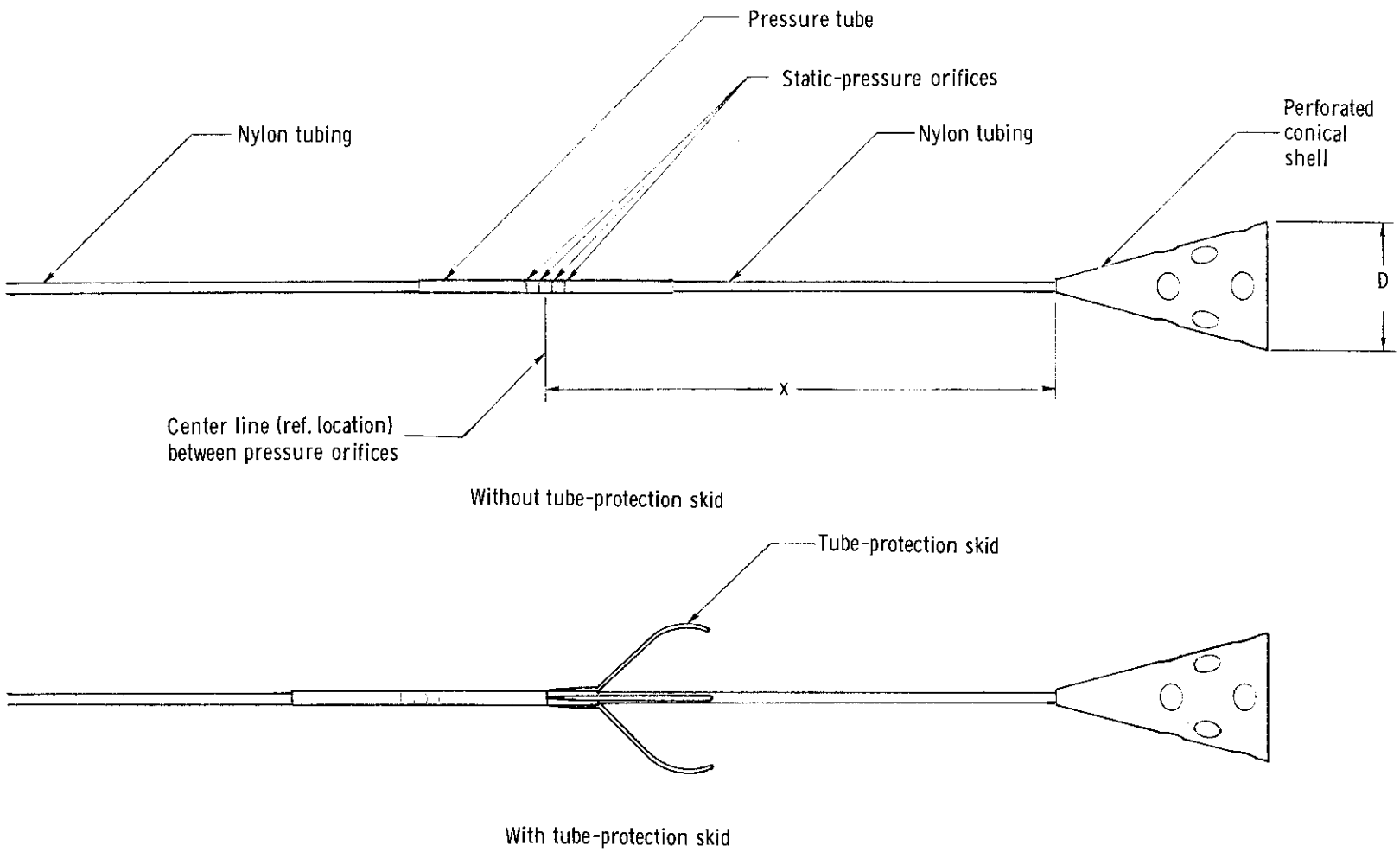

(a) Assembly view of trailing-cone device without and with tube-protection skid.

Figure 1.- Details of trailing-cone device for sensing static pressure. Dimensions are in centimeters (inches).

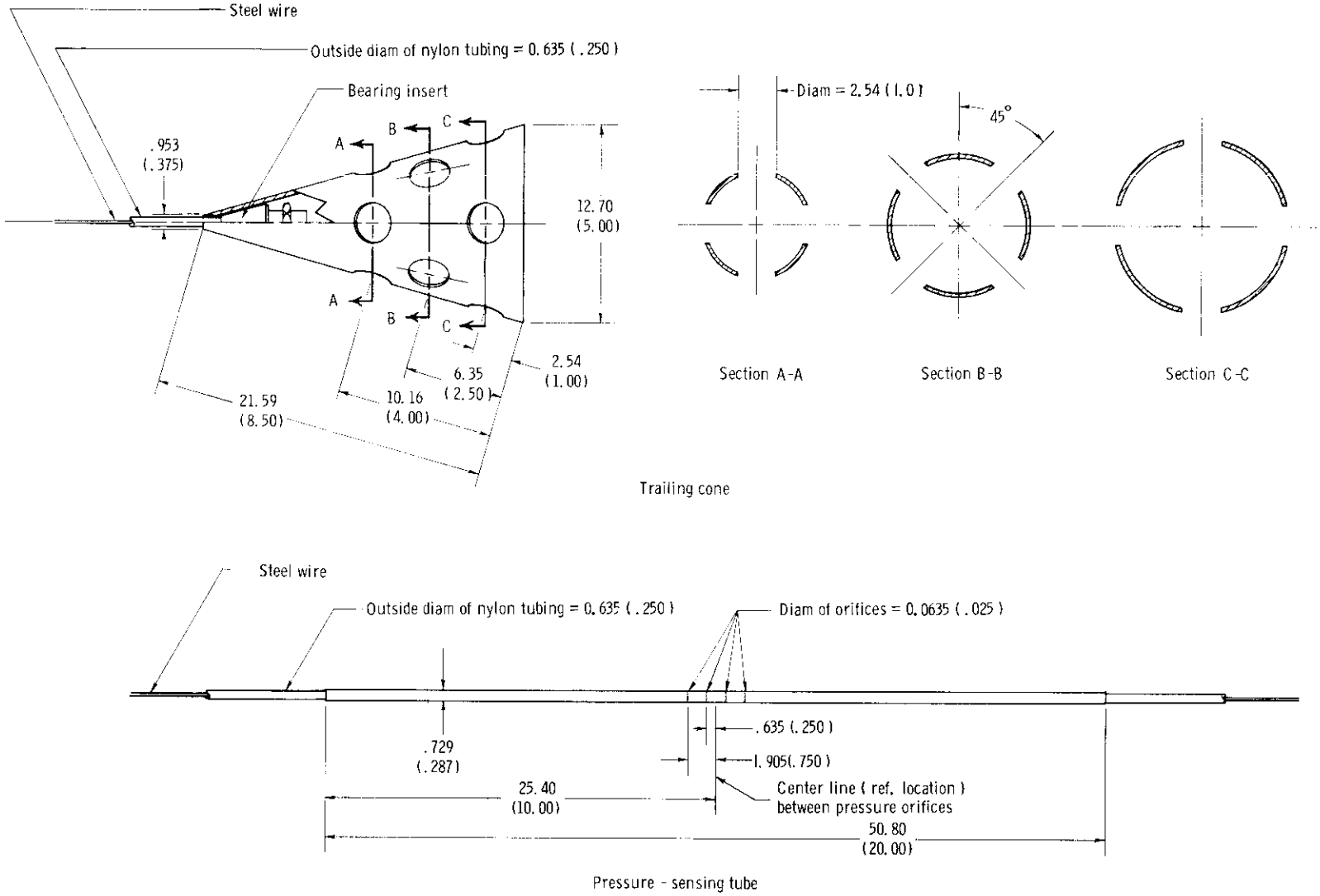

(b) Cone and pressure tube.

Figure 1.- Continued.

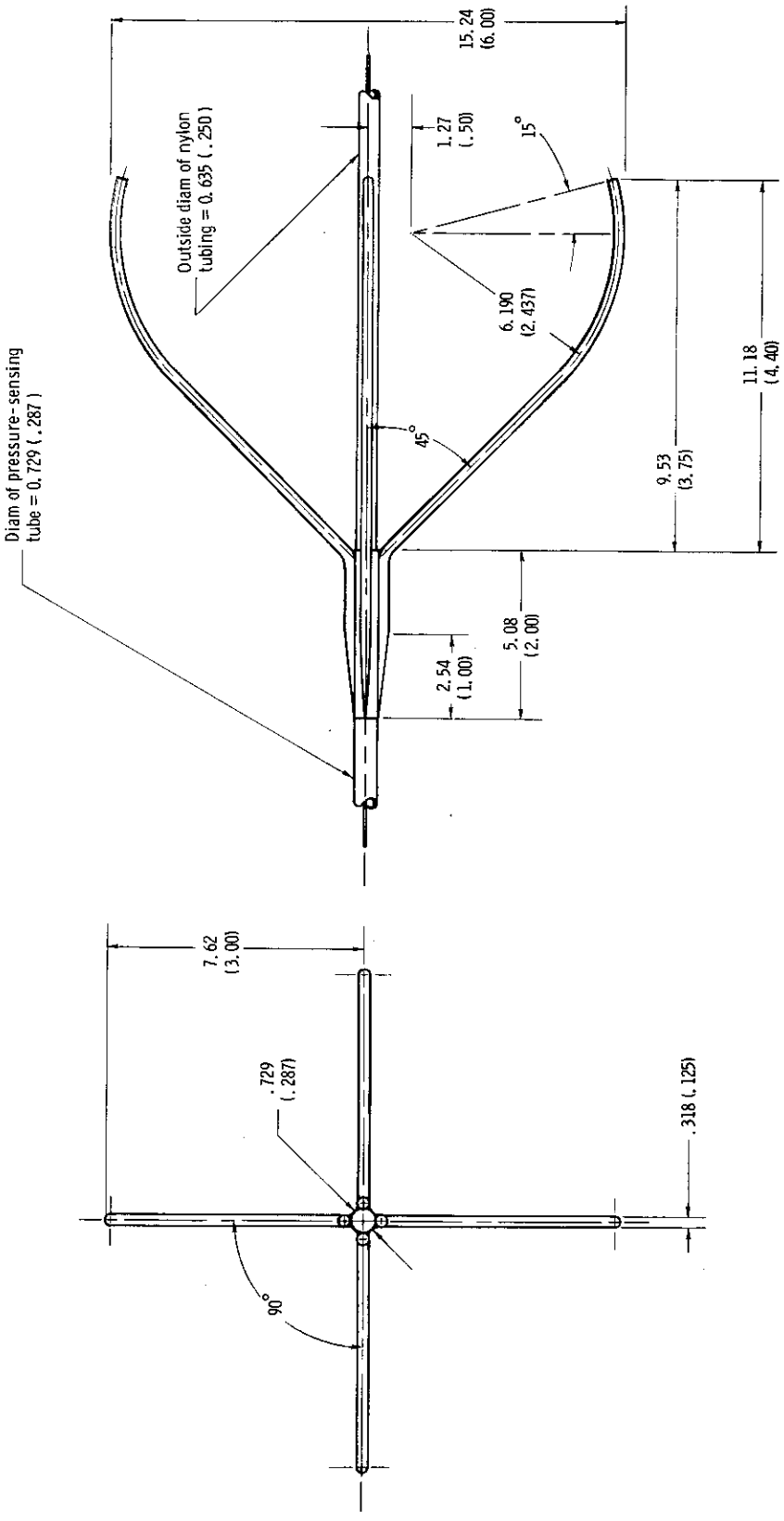

(c) Tube-protection skid.

Figure 1.- Concluded.

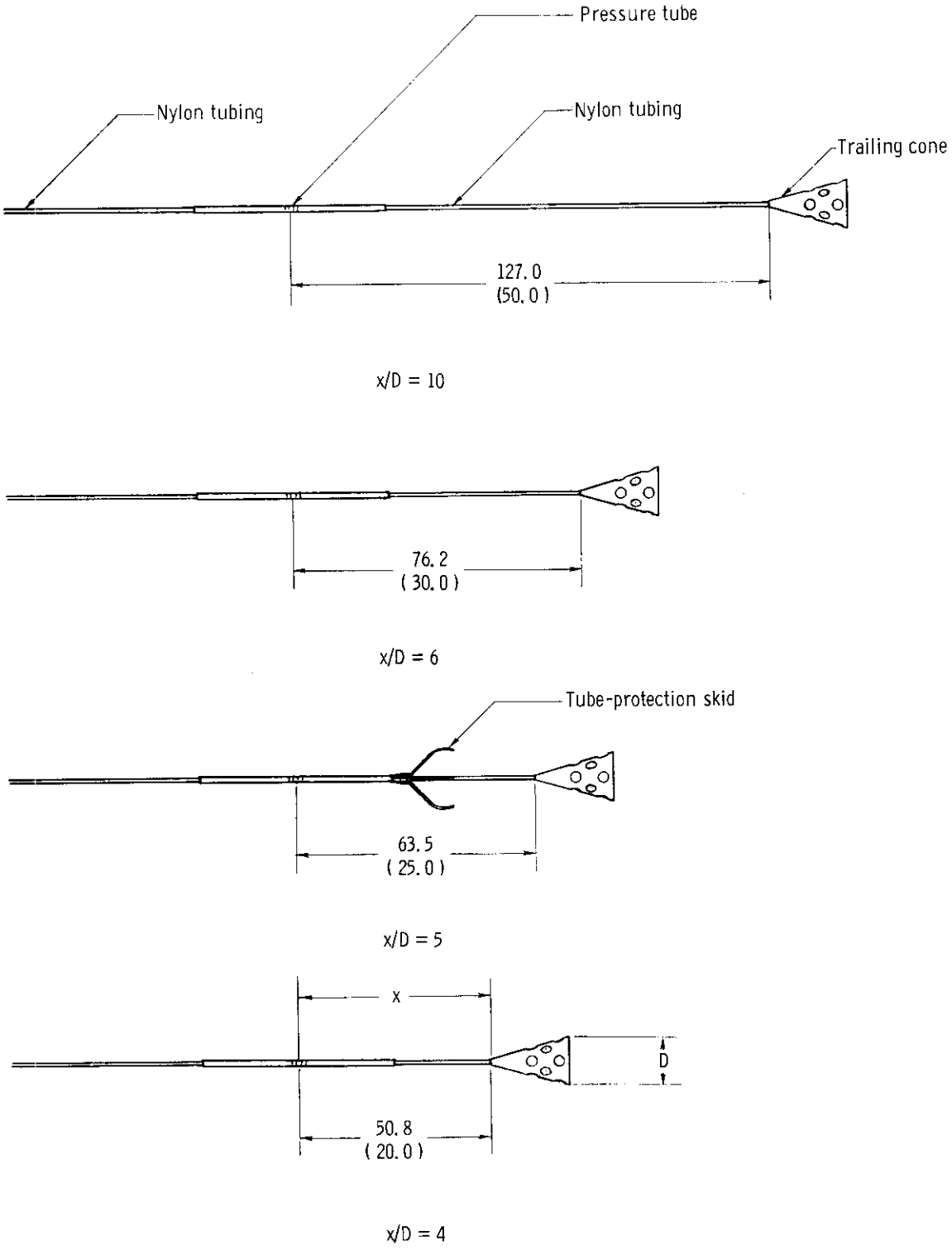

Figure 2.- Trailing-cone configurations tested. Dimensions are in centimeters (inches).

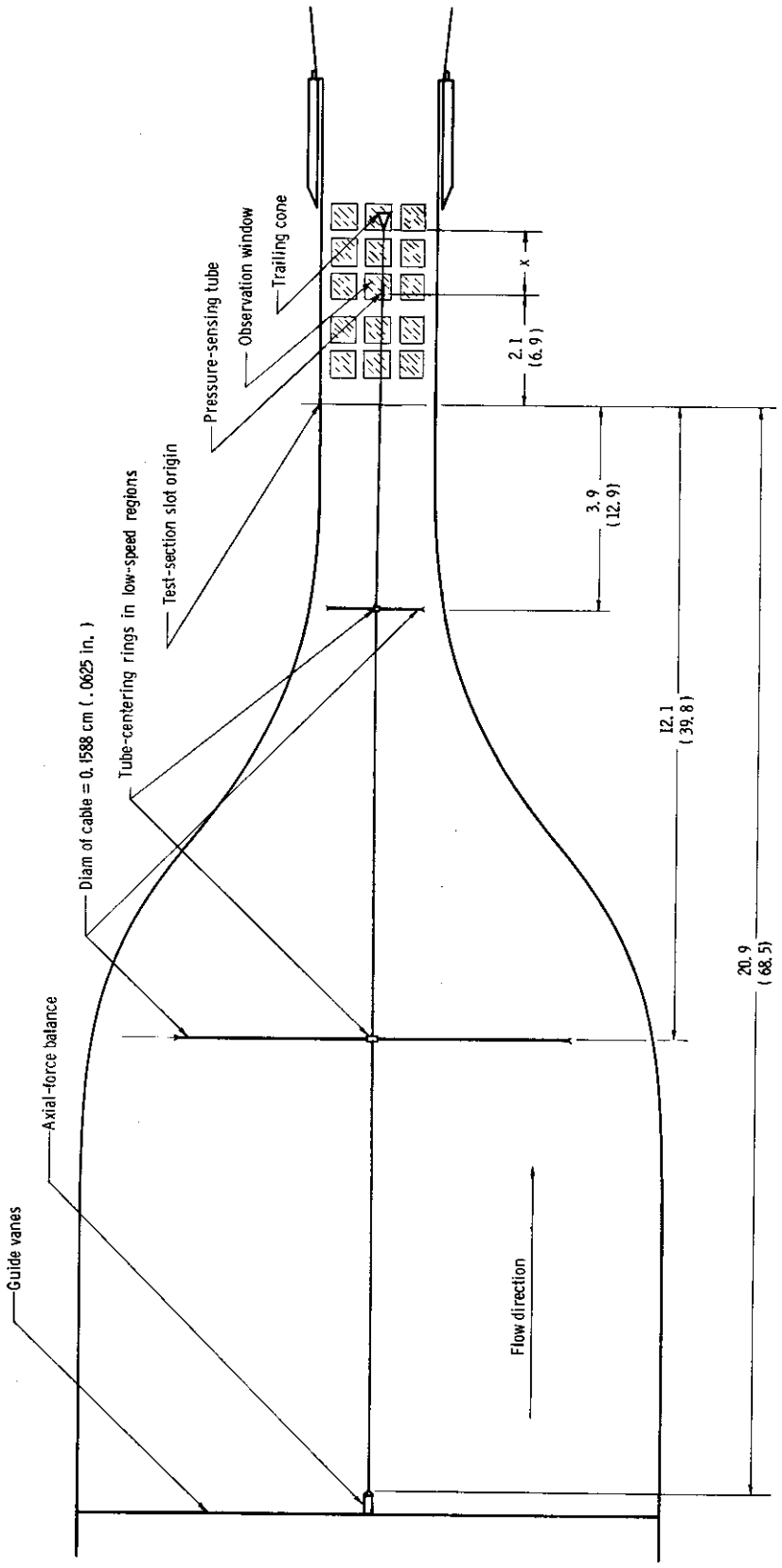

Figure 3.- Principal details of test arrangement. Dimensions are in meters (feet) unless otherwise noted.

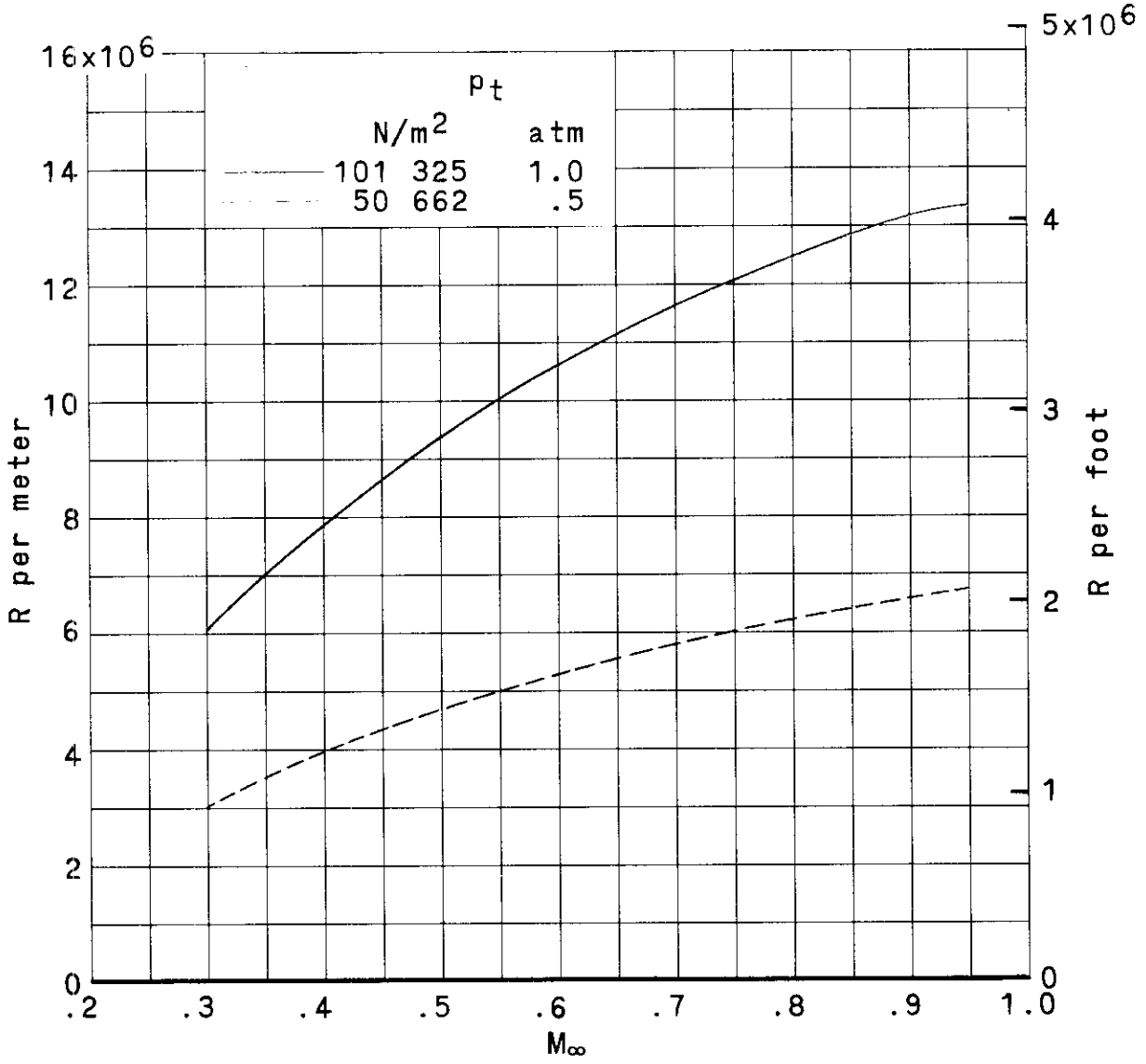

(a) Reynolds number.

Figure 4.- Variation of test Reynolds number and simulated pressure altitude with Mach number.

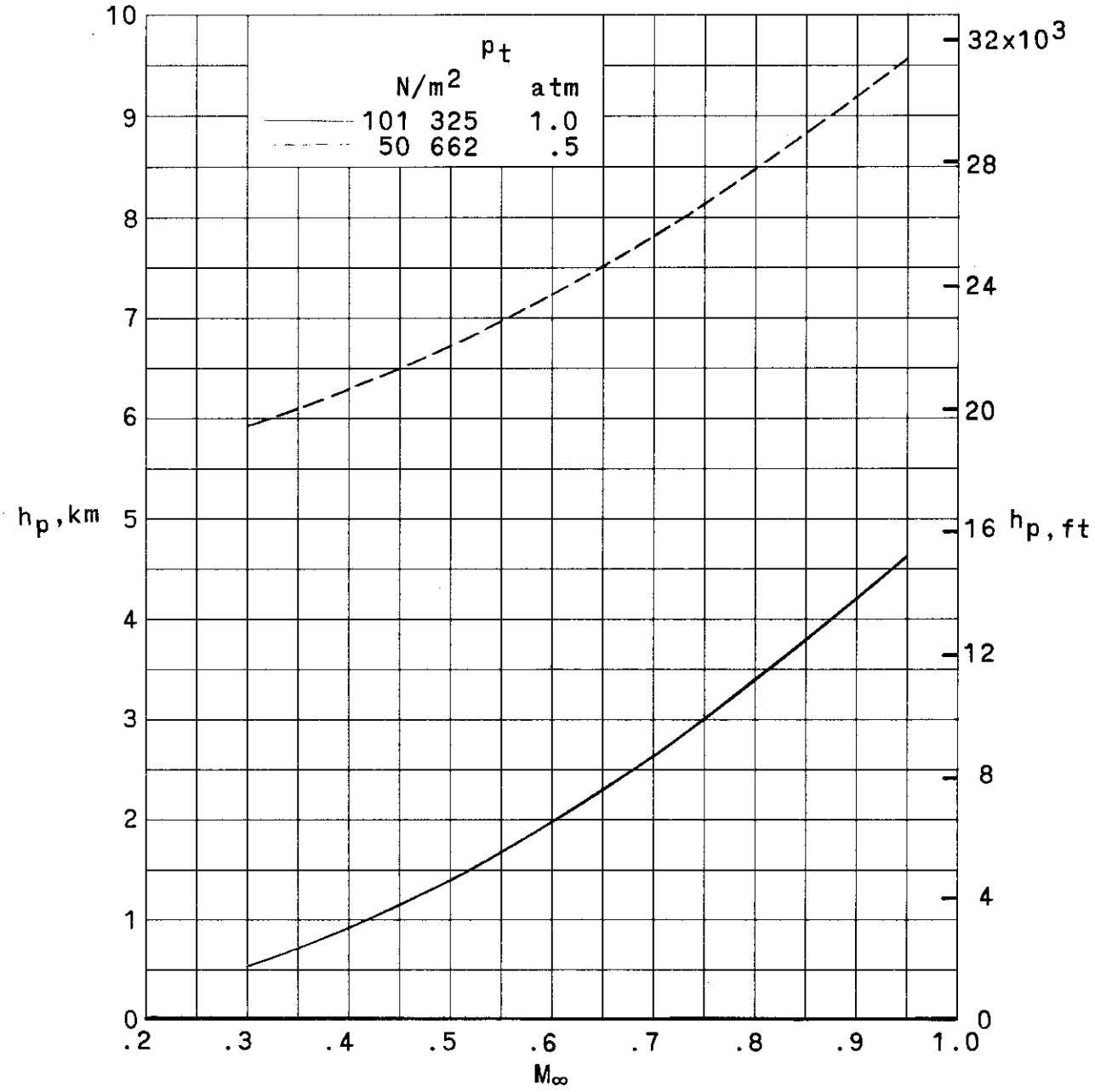

(b) Simulated pressure altitude.

Figure 4.- Concluded.

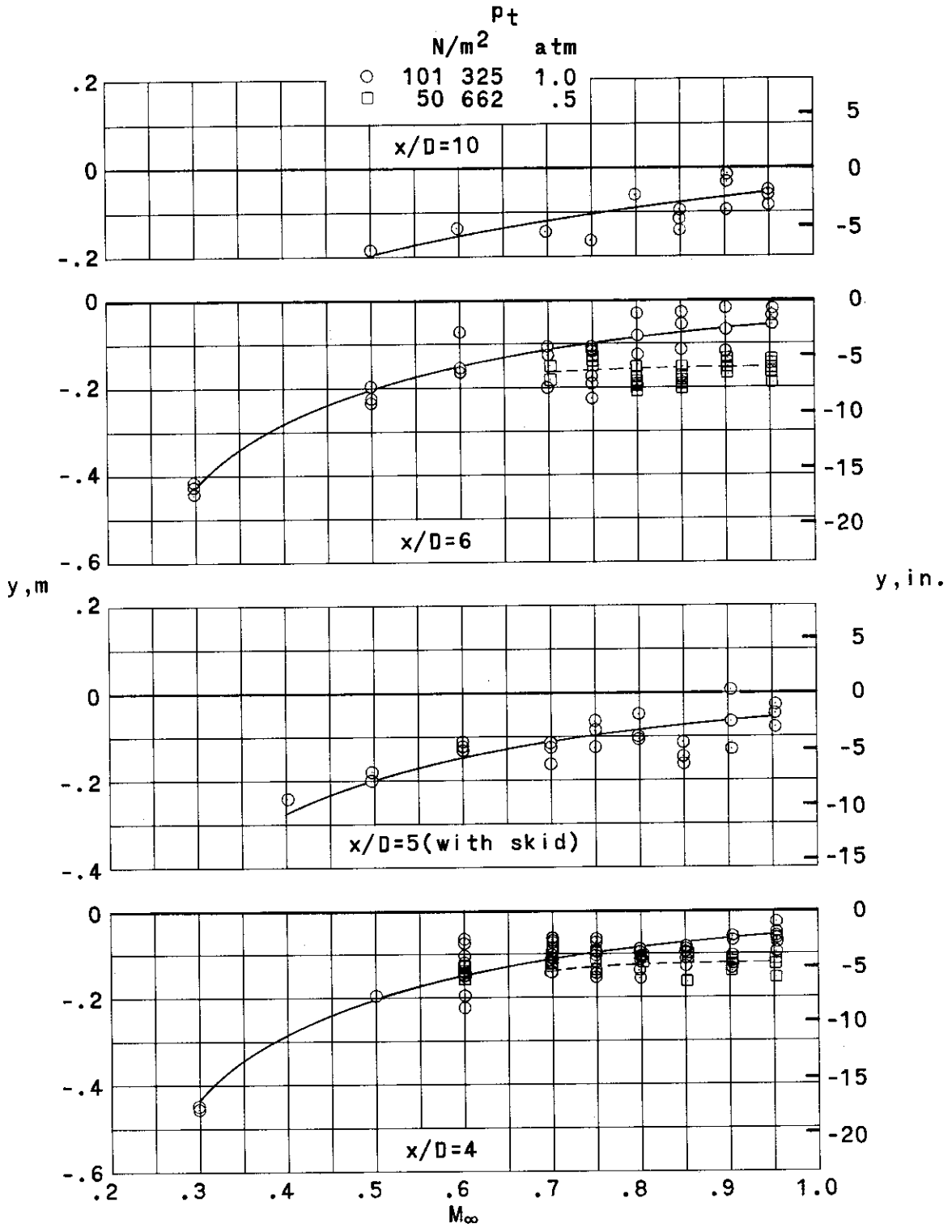

Figure 5.- Deviations of pressure-tube locations from test-section center line.

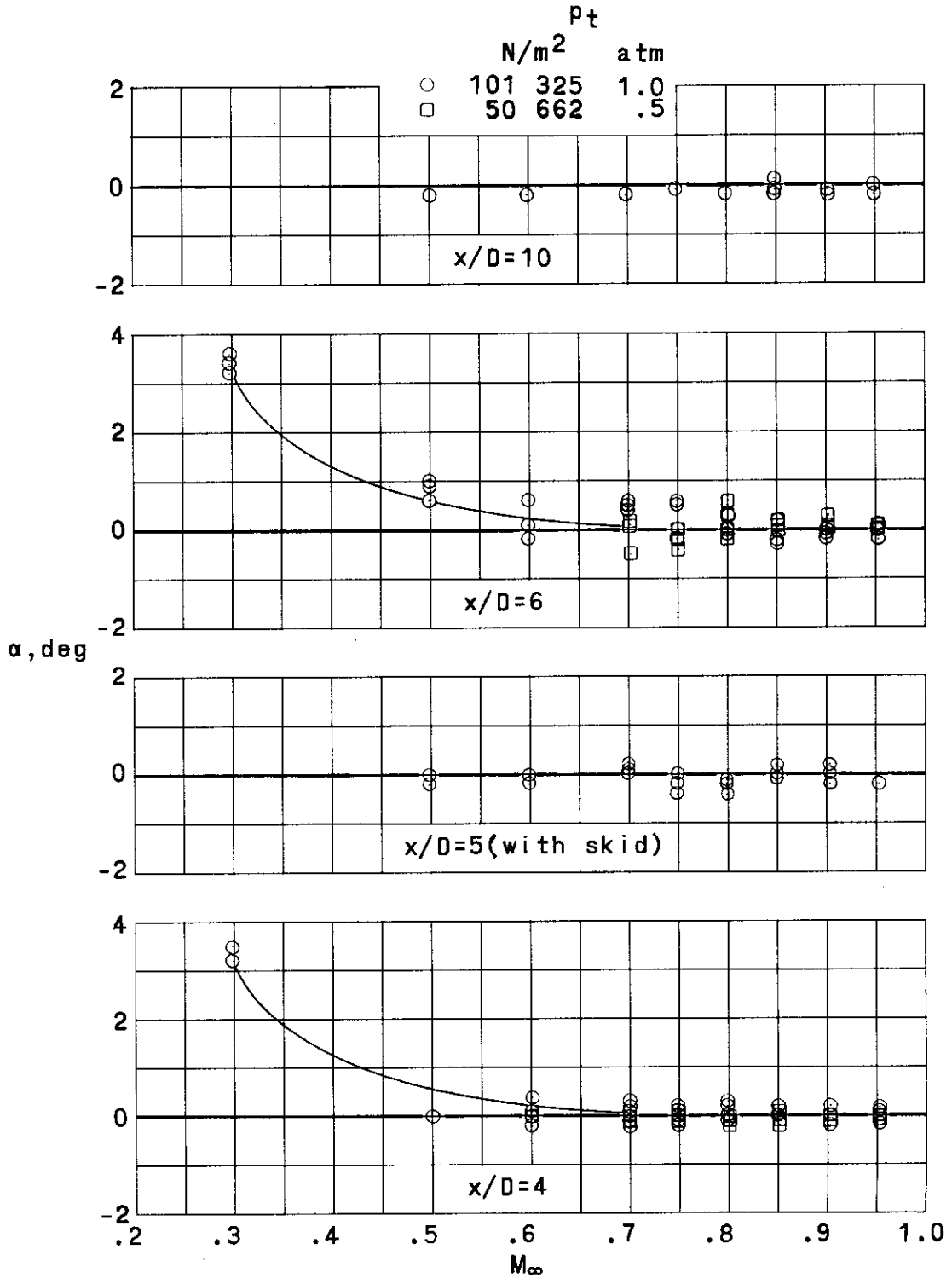

Figure 6.- Variation of pressure-tube angle of attack.

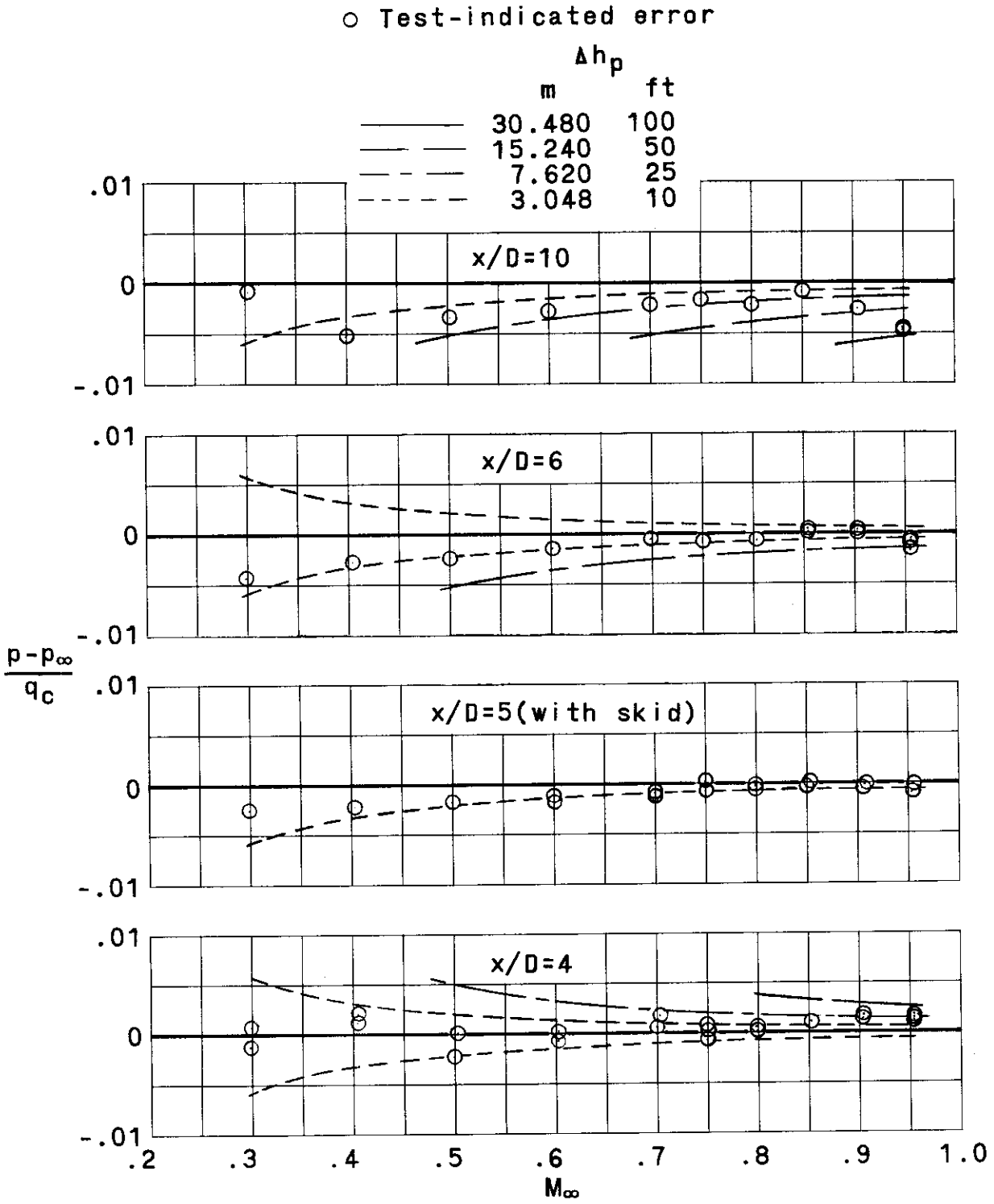

(a) Error expressed in terms of impact pressure and corresponding changes in pressure altitude.

Figure 7.- Static-pressure error indicated by trailing-cone device during subsonic tests at a total pressure of 1.0 atm.

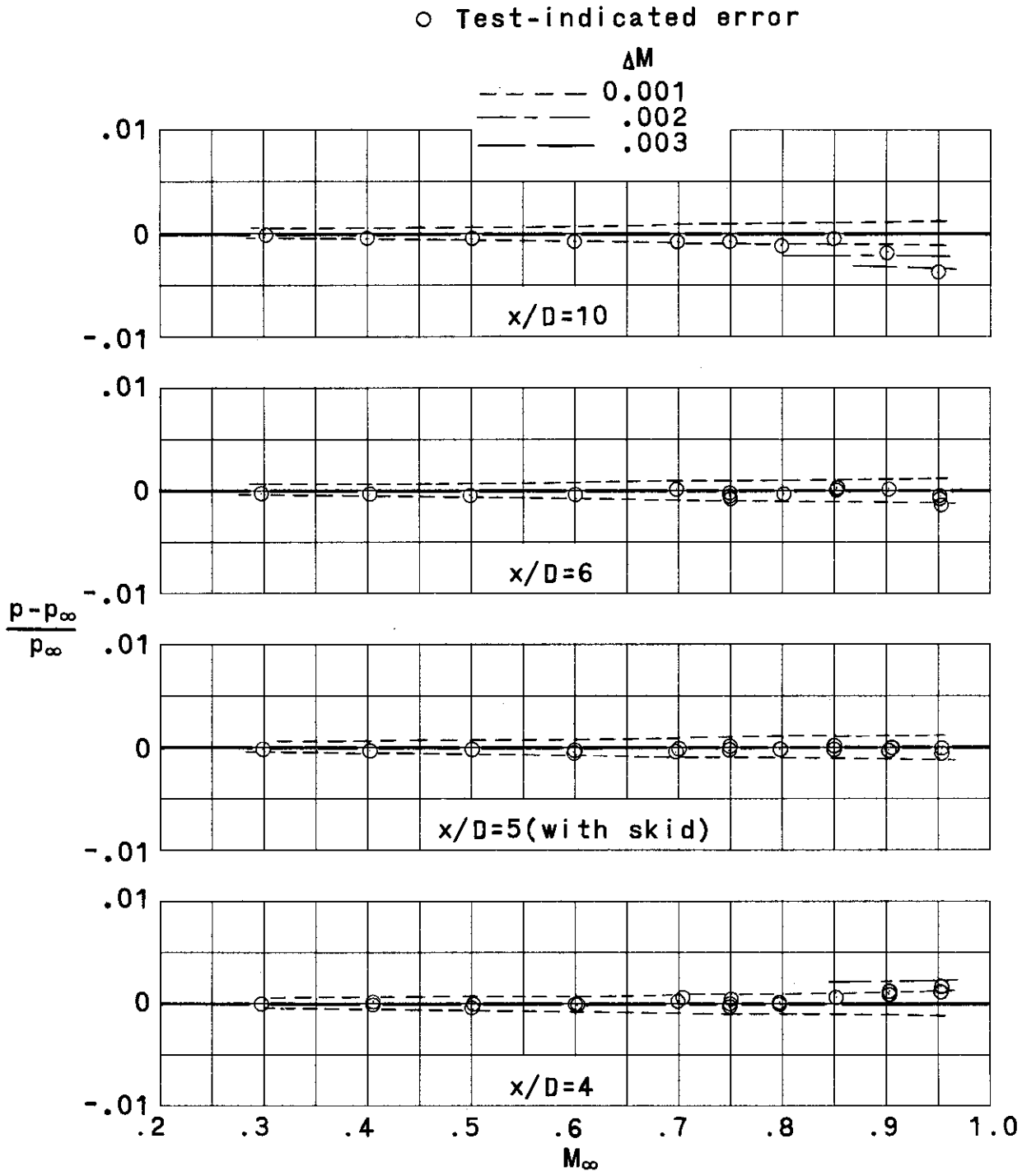

(b) Error expressed in terms of free-stream static pressure and corresponding changes in Mach number.

Figure 7.- Concluded.

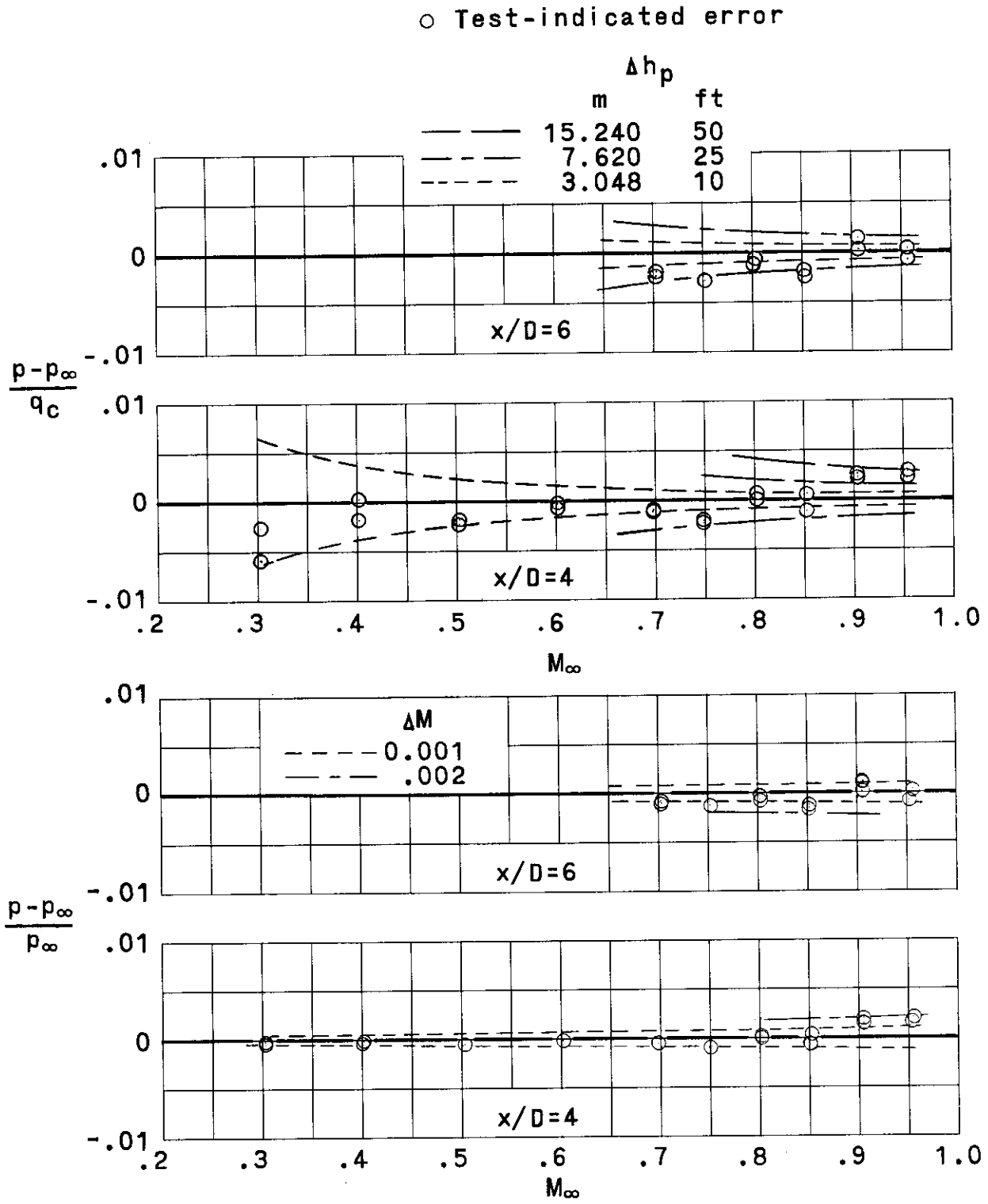

Figure 8.- Static-pressure error indicated by trailing-cone device during subsonic tests at total pressure of 0.5 atm. (Error is expressed in terms of impact and free-stream static pressures as well as corresponding changes in pressure altitude and Mach number.)

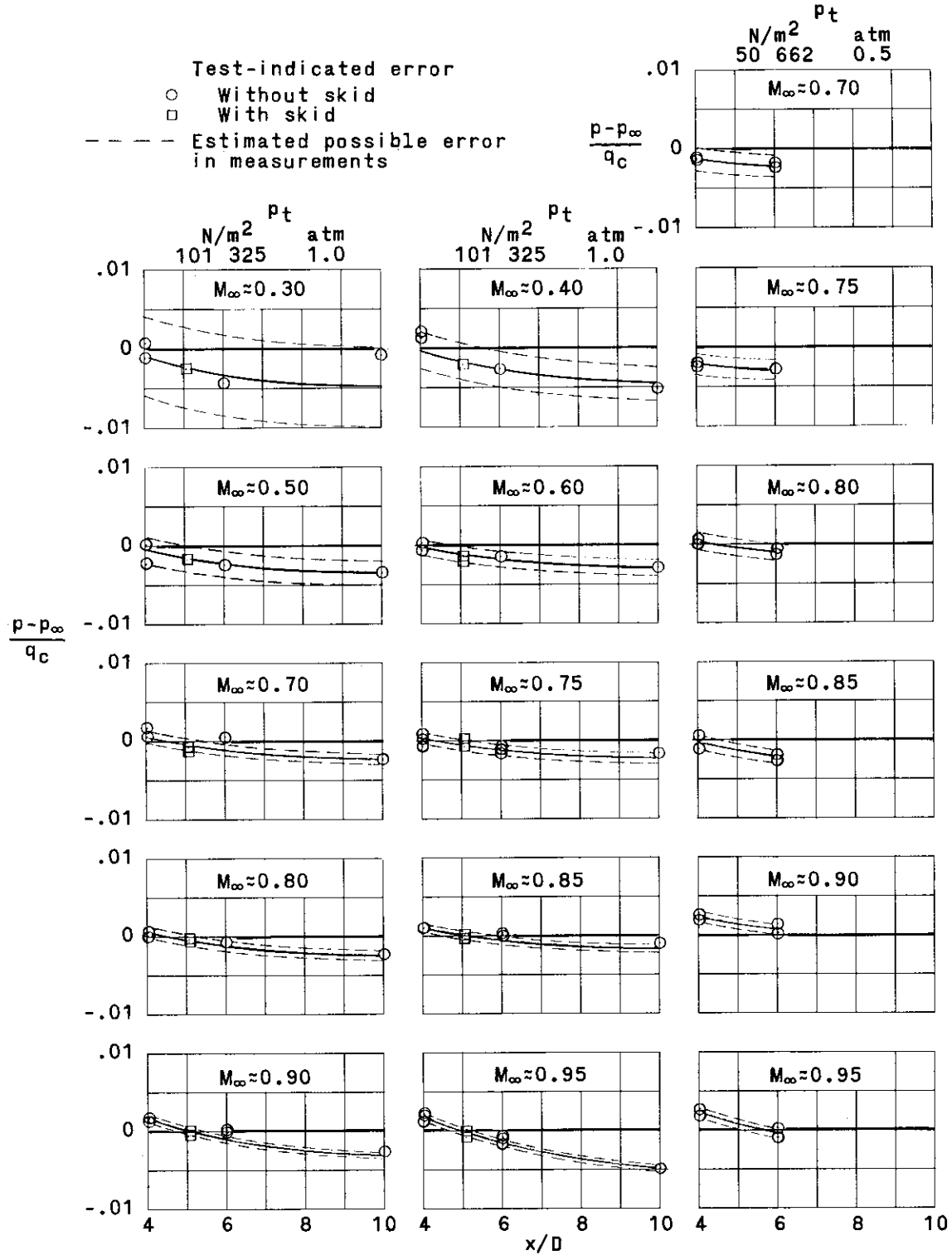

Figure 9.- Variation of static-pressure error for the trailing-cone device with changes in the distance between the pressure orifices and the cone. (Error is given in terms of impact pressure at total pressures of 1.0 and 0.5 atm.)

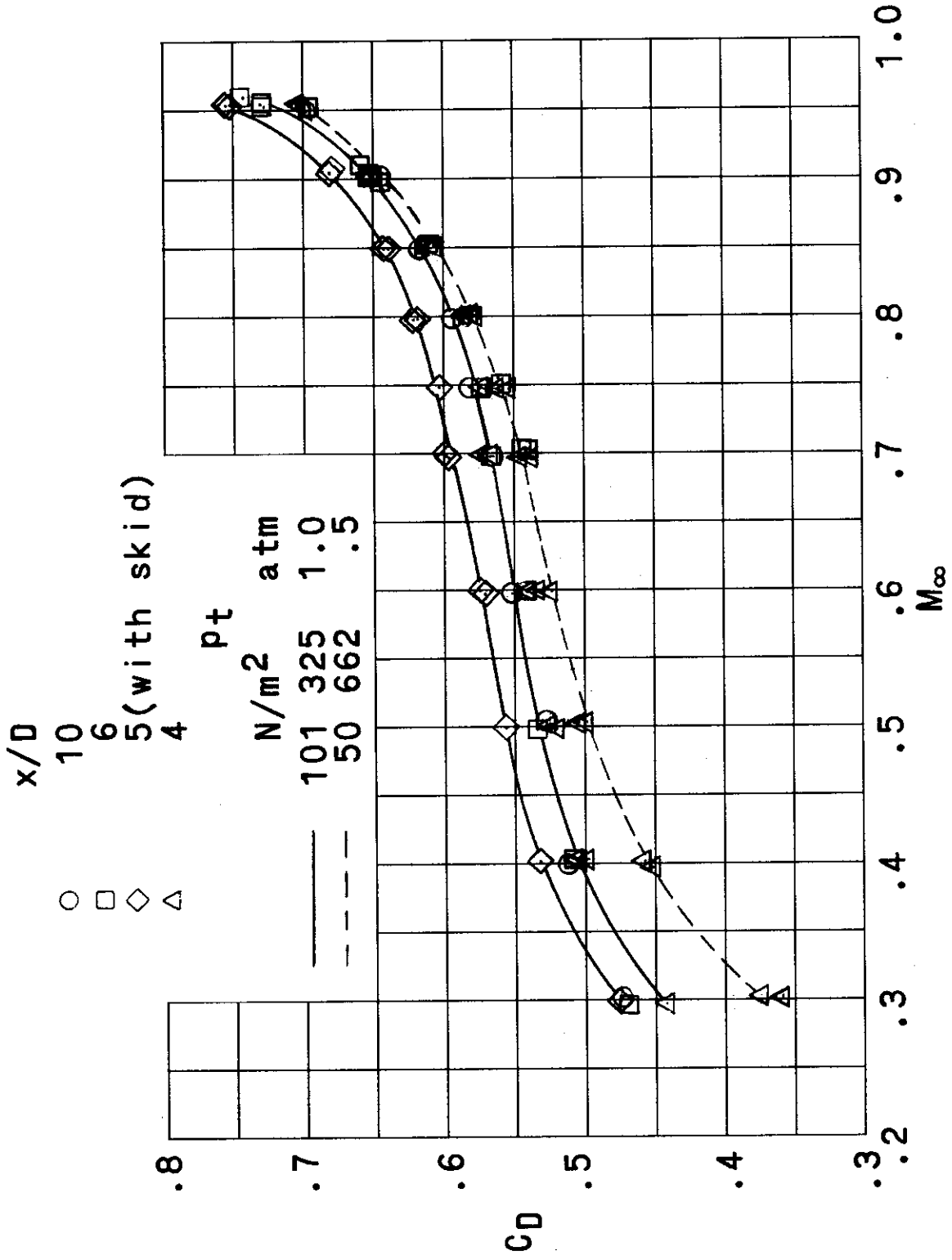

Figure 10.- Drag characteristics of trailing-cone configurations.